Long-period fiber gratings fabricated by use of defocused CO_2 laser beam for polarization-dependent loss enhancement

Minwei Yang, Yuhua Li, and D. N. Wang*

Department of Electrical Engineering, The Hong Kong Polytechnic University, Hung Hom, Kowloon, Hong Kong, China
**Corresponding author: eednwang@polyu.edu.hk*

Received January 23, 2009; revised March 17, 2009; accepted April 8, 2009; posted April 21, 2009 (Doc. ID 106665); published May 12, 2009

An alternative of the long-period fiber grating (LPFG) fabrication method has been developed in this work by use of defocused CO_2 laser pulse scanning, which is achieved by moving the laser beam focus plane slightly away from the fiber cladding surface. By increasing the distance shift from the cladding surface, the area with refractive index change also increases on the side with laser irradiation, which leads to an apparent mode field profile distortion at the resonant wavelength of the LPFG. Such a distortion in the mode field profile significantly increases the polarization-dependent loss of the LPFG. Moreover, for the cascaded LPFGs fabricated by use of this technique, the maximum polarization-dependent loss obtained can be largely increased from 7 to 17.8 dB, with a maximum dip in the wavelength change of 0.45 nm.
OCIS codes: 050.2770, 060.2340, 230.5440, 280.4788.

1. INTRODUCTION

Long-period fiber grating (LPFG) has been widely used in various kinds of optical communication devices and optical fiber sensors because of its capability of performing power coupling between core modes and codirectional cladding modes at resonant wavelengths [1]. One simple and convenient method of LPFG fabrication is the use of a CO_2 laser beam to irradiate single-mode optical fibers [2–5], which requires the laser focus to be located in the fiber cladding, and the fabricated LPFG possesses a polarization-dependent loss (PDL) of around 1 dB.

Recently, the in-fiber polarizer based on LPFG has received more and more attention. For example, such a device can be used as an in-line fiber polarizer [6] or a wavelength switching element in a fiber ring laser [7]. Meanwhile, different types of fibers, including polarization maintaining fibers, photonic crystal fibers, and hollow-core photonic bandgap fibers, have been used to make such devices [7–9]. The main reason for the polarization dependency is the asymmetric stress relief due to the one-sided laser irradiation.

In this paper we report a new alternative to increase the PDL of the LPFG fabricated in a normal single-mode fiber by use of defocused CO_2 laser pulses, i.e., to move the laser focus plane away from the fiber surface for a small distance (hereafter denoted as the defocused length). The LPFG obtained by use of this method possesses a relatively large PDL when compared with that obtained by conventional methods, which means that it can be effectively used as a polarization-sensitive element. Meanwhile, the mode field profile obtained at the corresponding resonant wavelength shows that with the increase of the defocused length, the cladding area affected by the laser energy also increases, which results in the distortion of the mode field profile and thus an increase of the PDL. The experimental results obtained in this work show that the PDL of the device can be further enhanced when a cascaded LPFG (CLPFG) structure is adopted. Moreover, the change of the residual stress relaxation profile in the fiber cross section as a possible mechanism for such PDL enhancement and mode distortion is discussed.

2. FABRICATION PROCESS AND PDL TEST

The experimental setup is shown in Fig. 1. A high-frequency CO_2 laser system (Han's Laser) with wavelength of 10.6 μm, repetition rate of 10 kHz, and average output power of ~0.5 W under computer control is used to scan the fiber. An optical spectrum analyzer (Ando AQ6319) and a light-emitting diode source are used to observe the transmission spectrum. The standard single-mode fiber is accurately positioned using a translation stage that can adjust the distance between the fiber surface and the laser focus plane. One of the fiber ends is fixed on the translation stage, and a small weight clog (~5 g) is hung on the other free end to ensure that the fiber is straight during the fabrication. The laser pulses first scan along the perpendicular direction of the fiber (y direction) and then shift to a grating pitch along the fiber length (x direction) before the next scan starts. The process continues until the whole grating length is reached, which forms a complete cycle. Usually several cycles are needed to write an LPFG with large resonant peak amplitude. The same laser output power is employed for different scanning cycles by keeping the control parameters unchanged.

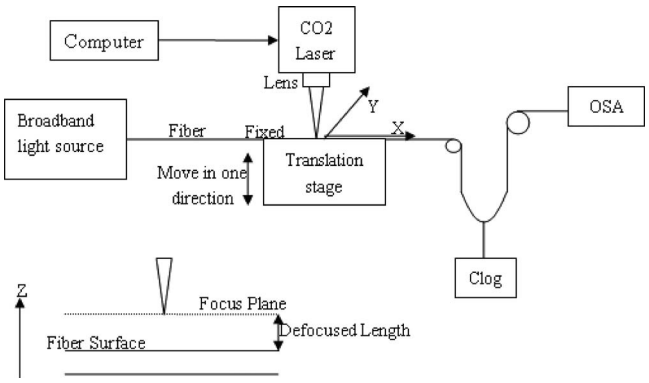

Fig. 1. Fabrication of LPFG with defocused high-frequency CO_2 laser.

Figure 2 shows the surface figures captured by a CCD (STC-P63CT), which corresponds to the defocused length of 0, 1, and 2 mm, respectively. Each of the three LPFGs has a grating pitch of 400 μm and a grating number of 40. The CO_2 laser has a focused-beam spot diameter of 35 μm [4], which means that the laser beam irradiation cannot reach the whole fiber surface when it is accurately focused. When the defocused length is small, the laser can carve periodical grooves on the cladding due to the high local temperatures created [4], as shown in Figs. 2(a) and 2(b) respectively. It should be noticed that since the air gap introduces a certain loss of laser energy, the larger the defocused length, the more scanning cycles are needed to write LPFGs with similar resonant depth. For instance, the three samples here require scanning cycles of 7, 15, and 80, respectively. During the scanning process, no over-coupling appears in these samples.

The PDL test results and the polarization-induced minimum and maximum transmitted power of the three samples are shown in Fig. 3. The test system includes a tunable laser (Agilent 8164B), a polarization controller (Agilent 8169A), and an all-parameter analyzer (Agilent 81910A), which are all controlled by the software during the test procedure. The PDL is calculated by means of the Mueller matrix method [10]. The LPFG written by the focused light beam possesses a maximum PDL of 1.10 dB, which is similar to that with large dimensional grooves (1.35 dB) [4] and edge-written (originally 1.22 dB) LPFG [5]. However, by applying the defocused laser beam for scanning and increasing the defocused length, the maximum PDL is greatly increased to 3.68 dB (for 1 mm) and 4.38 dB (for 2 mm), respectively. The polarization-induced dip changes of the three samples are 0.19, 0.95, and 0.6 nm, respectively. The three LPFGs have similar values of a single-side 3 dB stop bandwidth of 32.46 nm, 32.53 nm, and 30.55 nm, respectively, which indicates that the PDL difference among them is mainly due to the different levels of photo-induced birefringence in the fiber.

3. MODE FIELD DISTRIBUTION AT THE RESONANT WAVELENGTH

According to the phase-matching condition, LPFG couples energy from the fiber core to the fiber cladding, thus exciting a corresponding cladding mode at the resonant wavelength. This cladding mode is typically a circularly

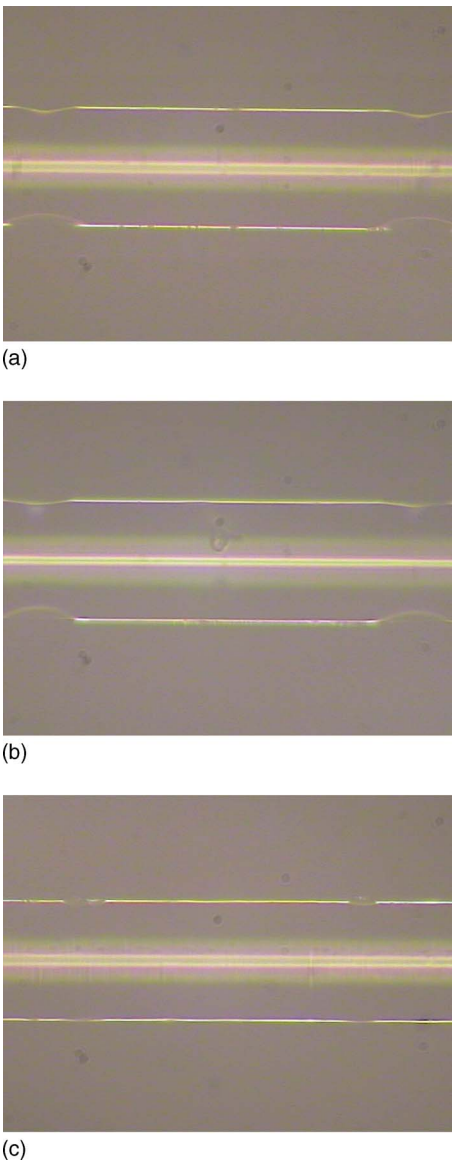

Fig. 2. (Color online) CCD figures of the cladding surface for LPFGs made by different defocused lengths (a) 0 mm, (b) 1 mm, (c) 2 mm.

symmetric mode (LP_{0x}) when the refractive index (RI) change locates mainly in the fiber core. However, in the case of a large asymmetric RI change in the fiber cross section, a circularly asymmetric cladding mode (LP_{1x}) can also be excited [11,12] and thus can form a hybrid mode coupling. The mode field profile is related to the magnitude of the RI change in the fiber cross section [11]. The near-mode profiles at the resonant wavelengths of the three different LPFGs have been examined in order to find the relationship between the increase of the PDL and the defocused length.

The system for observing the LPFG near-mode field profile includes a tunable laser (Agilent 8164B), a lens, an infrared camera (Electro Physics 7290A), and a data-collecting computer. The output power of the tunable laser is kept constant during the whole experiment. The tested LPFG is perpendicularly cleaved at one end of the grating length in order to observe the near-field profile.

The brightness of the mode field profile is proportional to the mode energy intensity, which is related to the level of RI change.

Figure 4 shows the near-mode profile of each LPFG at its corresponding resonant wavelength. It can be observed that, when the focus plane is accurately located on the cladding surface, the excited cladding mode field has a strong angle-dependent profile, as shown in Fig. 4(a). The intensity of the profile also implies that the RI change is mainly concentrated along the laser irradiation direction. Since the grating length is relatively small (16 mm), the cladding mode field profile is mainly a circularly asymmetric LP_{16} mode superimposed with other cladding modes.

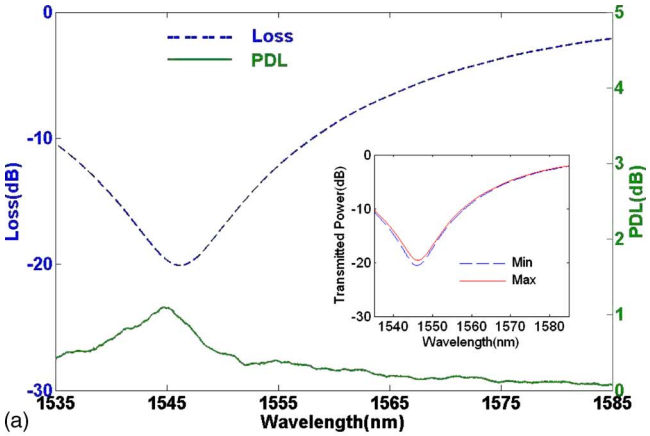

(a)

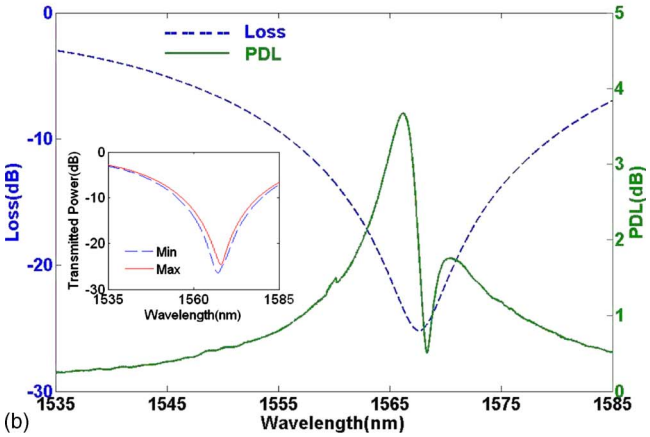

(b)

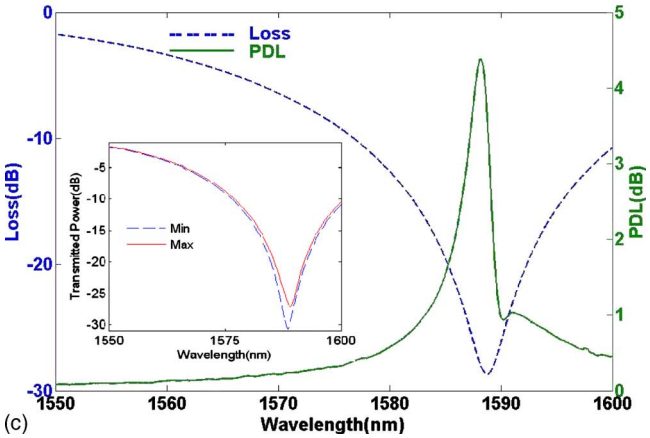

(c)

Fig. 3. (Color online) PDL test of LPFGs with defocused lengths (a) 0 mm, (b) 1 mm, (c) 2 mm.

The near-mode field profiles (at the resonant wavelength) of the other two samples are shown in Fig. 4(b) and Fig. 4(c), respectively. The cladding mode changes from a single-side hybrid modelike profile to a standard LP_{16} modelike profile. Moreover, since the output power of the tunable laser (or the input power of the three samples) is the same, the mode field intensity implies that more power is confined to the area near the core as the defocused length increases.

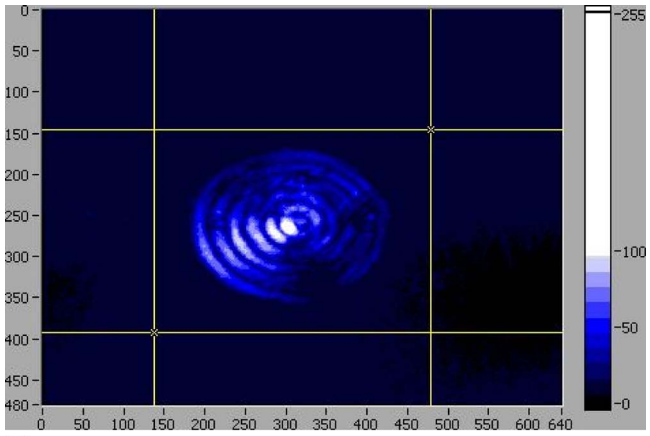
(a)

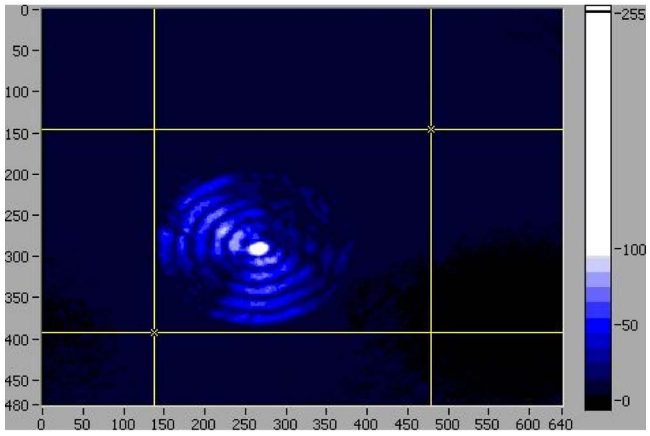
(b)

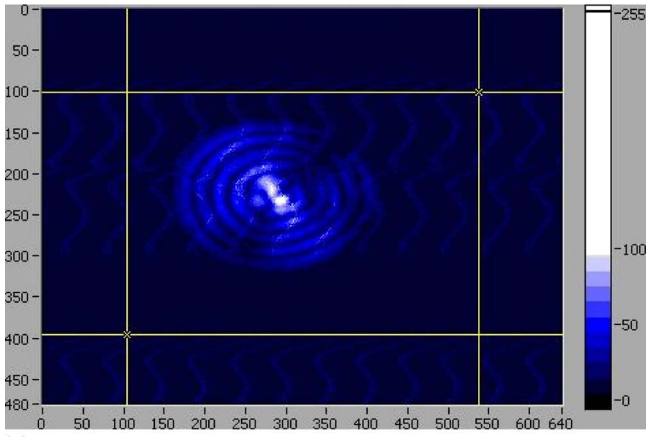
(c)

Fig. 4. (Color online) Mode distortion of excited cladding mode of LPFGs with defocused lengths (a) 0 mm, (b) 1 mm, (c) 2 mm.

4. CLPFG FABRICATED BY THE DEFOCUSED CO_2 LASER AS A POLARIZATION SENSITIVE ELEMENT

Since a single LPFG usually has a large resonant depth and a broad stop bandwidth, the applications of its PDL are limited in the fields of optical sensing or wavelength tuning. However, if two LPFGs are cascaded, the device behaves like a Mach–Zehnder interferometer and thus the PDL can be significantly increased due to the cascaded enhancement effect [13] and the high-finesse interference fringe [14]. Such a large PDL achieved in cascaded LPFGs (CLPFGs) is attractive in a fiber ring laser wavelength switch [13], multichannel system filter [14], and optical sensing [15].

We have fabricated a CLPFG with enhanced PDL by use of a defocused CO_2 laser beam. The fabrication procedure is much the same as that shown in Fig. 1 except that two 2-D translation stages are used to move the fiber in the x direction. When the first 3 dB LPFG is created (actually, the resonant depth is slightly larger than 3 dB when considering the insertion loss), the fiber needs to be shifted a certain distance (22 cm, or the cascaded fiber length) before writing the second one. Each LPFG has a grating pitch of 385 μm and a period number of 30. As shown in Fig. 5, an upper envelope exists in the transmission spectrum [the symbols (a) and (b) indicate the defocused length of 0 and 2 mm, respectively]. Two reasons for the deterioration of the interference spectrum are: i) we can hardly avoid the small deviation of the laser irradiating direction for the two gratings as the cascaded fiber is relative long, and ii) the cladding mode excited in the first LPFG may suffer a certain amount of transmitted loss in the cascaded fiber. The maximum PDL for each CLPFG is 7.0 dB and 17.8 dB, respectively (the latter is larger than that reported in [14], which is ~10 dB for two cascaded LPFGs). This PDL corresponds to the maximum dip wavelength shifts of 0.15 and 0.45 nm, respectively. The polarization-induced minimum and the maximum transmitted power of both the two CLPFGs are also shown in Fig. 5(c) and Fig. 5(d). The result implies that both the PDL and the maximum dip shift increases with the increase of defocused length. Besides, the maximum dip shift of 0.45 nm is larger than that reported in [13,14].

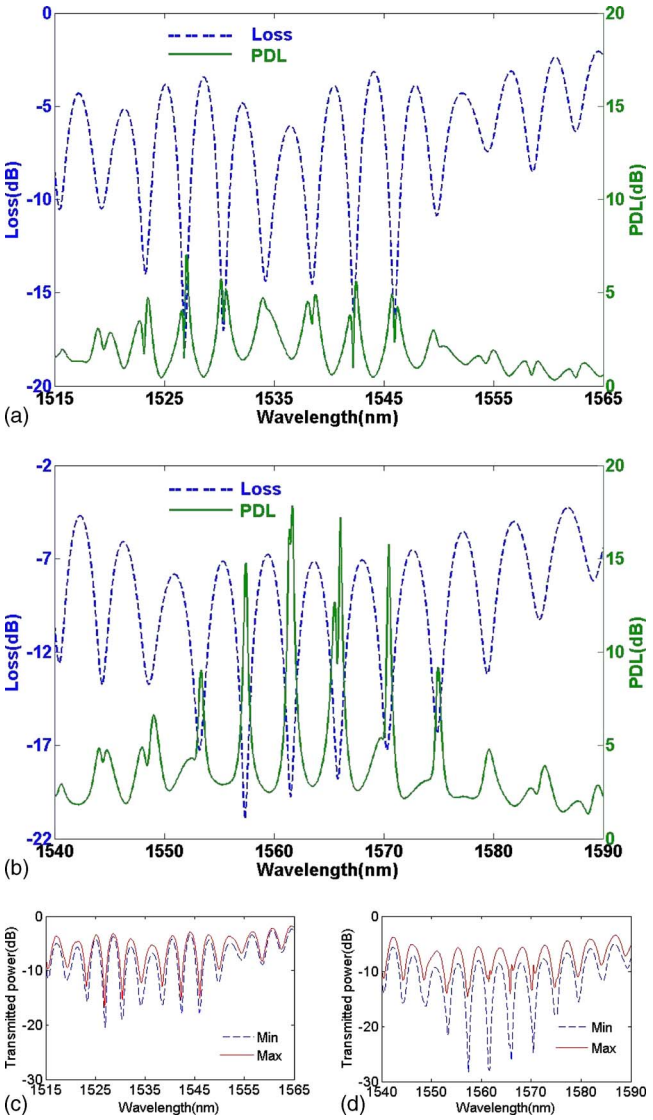

Fig. 5. (Color online) PDL test of CLPFGs with different defocused lengths (a) 0 mm and (b) 2 mm, and the polarization-induced minimum and maximum transmitted power of CLPFGs with different defocused lengths (c) 0 mm and (d) 2 mm.

5. DISCUSSION

Since a small CO_2 laser average output power of ~0.5 W and a small tension (~5 g) are used during the scanning process, the periodic residual stress relaxation is considered to be the main mechanism to form the grating. When the focus plane is moved away from the cladding surface, both the transmission loss in the air and the enlargement of the affected area will lower the power density irradiated on the cladding surface. This in turn reduces the laser penetration depth into the fiber, thus decreasing the heat depth of the silica glass [16]. This implies that the residual stress relaxation mainly occurs near the cladding surface region in the laser irradiation direction, while the fiber core is hardly affected.

Since relaxation of the mechanical residual stress is the main cause for the RI change, both the effective RI of the cladding mode ($n_{eff,cl}$) and the core mode ($n_{eff,co}$) are decreased under the focused CO_2 laser irradiation [17]. Being different from that of the LPFG written with a focused light beam [2,17,18], the asymmetric change in the stress relaxation distribution profile of the fiber cladding cross section is the main reason for the enhancement of the polarization-dependent property [17]. In this situation, $n_{eff,cl}$ decreases while $n_{eff,co}$ changes little, as the RI change mainly occurs near the cladding surface. This results in the different resonant wavelengths of the three samples in Fig. 3.

Meanwhile, the RI change can also affect the near-field profile. For the normal penetration depth, the RI decreases linearly from the cladding surface to the core. However, when the penetration depth is small, the RI change may follow an approximately quadratic or exponential profile [11]. Based on this assumption, we simulate the corresponding LP_{16} cladding mode field in a normal SMF28 fiber with different side RI change profiles.

The expression for each of the profiles is: i) $n=n_0-y\Delta n_1$, ii) $n=n_0-y^2\Delta n_2$, and iii) $n=n_0-(e^{y/R}-1)\Delta n_3$, respectively ($n_0$ is the initial cladding RI; y is the axis parallel with the laser irradiation direction, with the origin at the core center; R is the cladding radius; and Δn_i represents the coefficient that ensures that all the profiles have the same largest magnitude of RI change of 3×10^{-4} at the cladding surface). The RI changes should happen in the upper part of the fiber cladding region and are decreased in the perpendicular direction from the top down to the cladding-core boundary ($R>y>$Rcore, where Rcore is the fiber core radius). The results obtained are shown in Fig. 6. The labels (a)–(d) denote none (unperturbed fiber), linear, quadratic, and exponential cladding RI change profiles of the fiber, respectively. The simulated results have a similar change tendency with the results shown in Fig. 4 and hence can qualitatively explain the relationship between the mode field distortion and the cladding RI change profile. This relationship can also be understood by the fact that the mode field tends to shift toward the position where a larger index exists. When compared with the linear profile, the latter two possess the cladding RI change that is mainly near the fiber surface, and therefore the cladding RI can be considered to be nearly circularly symmetric near the cladding–core boundary. Therefore, the mode fields of the latter two profiles tend to become standard LP_{16} modes, while the first profile has a strongly angle-dependent mode field.

Moreover, the simulation results demonstrate an increase in birefringence of the four-fold degenerated LP_{16} mode with 3×10^{-6}, 4×10^{-6}, and 7×10^{-6}, respectively. This increase in the cladding mode birefringence also contributes to the enhancement of the PDL in the LPFG written with side laser irradiation [19]. Besides, in Fig. 3, LPFG2 possesses a larger dip change than that of LPFG3 while its PDL is smaller. This may be partly explained by the fact that LPFG3 has a larger resonant depth (28.69 dB) than that of LPFG2 (25.20 dB). This difference may counteract the effect of PDL in the resonant dip change. Meanwhile, the resonant bandwidth and the light power coupled into the fiber from a certain polarization state may also affect the relationship between PDL and the wavelength separation, as mentioned in [19].

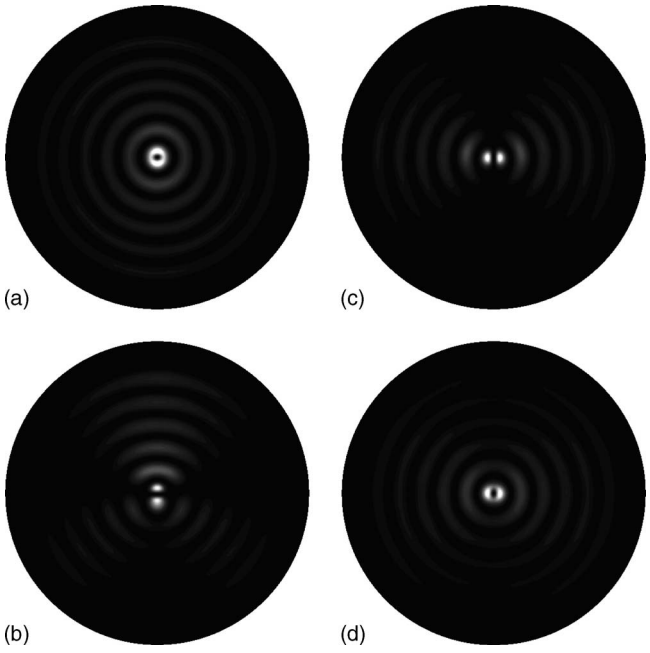

Fig. 6. Simulated LP_{16} mode profile with (a) none, (b) linear, (c) quadratic, and (d) exponential side cladding refractive-index change.

6. CONCLUSION

In conclusion, we have developed an alternative of the LPFG fabrication method by use of defocused high-frequency CO_2 laser pulse scanning. Such a technique can generate a relatively large PDL near the resonant wavelength in the grating, and the experimental results obtained can be explained by the distortion of the excited cladding mode field profile at the resonant wavelength. The possible mechanism for the enhancement of PDL may be due to the local refractive index change near the fiber cladding surface. Moreover, the CLPFG fabricated by this method exhibits a larger maximum dip wavelength shift and a greater PDL than that written by a focused CO_2 laser beam. The results obtained in this work have the potential to be used in an in-fiber polarizer at the resonant wavelength of the LPFG.

ACKNOWLEDGMENTS

This work was supported by the Hong Kong SAR government through General Research Fund grant 5291/07E.

REFERENCES

1. X. W. Shu, L. Zhang, and I. Bennion, "Sensitivity characteristics of long-period fiber gratings," J. Lightwave Technol. **20**, 255–266 (2002).
2. D. D. Davis, T. K. Gaylord, E. N. Glytsis, S. G. Kosinski, S. C. Mettler, and A. M. Vengsarkar, "Long-period fiber-grating fabrication with focused CO_2 laser pulses," Electron. Lett. **34**, 302–303 (1998).
3. Y. J. Rao, Y. P. Wang, Z. L. Ran, and T. Zhu, "Novel fiber-optic sensors based on long-period fiber gratings written by high-frequency CO_2 laser pulses," J. Lightwave Technol. **21**, 1320–1327 (2003).
4. Y. P. Wang, D. N. Wang, W. Jin, Y. J. Rao, and G. D. Peng, "Asymmetric long-period fiber gratings fabricated by use of CO_2 laser to carve periodic grooves on the optical fiber," Appl. Phys. Lett. **89**, 151105–151108 (2006).
5. T. Zhu, Y. J. Rao, J. L. Wang, and Y. Song, "A highly sensitive fiber-optic refractive index sensor based on an edge-written long-period fiber grating," IEEE Photon. Technol. Lett. **19**, 1946–1948 (2007).
6. A. S. Kurkov, M. Douay, O. Duhem, B. Leleu, J. F. Henninot, J. F. Bayon, and L. Rivoallan, "Long-period fiber grating as a wavelength selective polarization element," Electron. Lett. **33**, 616–617 (1997).
7. Y. W. Lee and B. Lee, "Wavelength-switchable erbium-doped fiber ring laser using spectral polarization-dependent loss element," IEEE Photon. Technol. Lett. **15**, 795–797 (2003).
8. H. F. Xuan, W. Jin, J. Ju, Y. P. Wang, M. Zhang, Y. B. Liao, and M. H. Chen, "Hollow-core photonic bandgap fiber polarizer," Opt. Lett. **33**, 845–847 (2008).
9. Y. P. Wang, L. M. Xiao, D. N. Wang, and W. Jin, "In-fiber polarizer based on a long-period fiber grating written on photonic crystal fiber," Opt. Lett. **32**, 1035–1037 (2007).
10. Y. P. Wang, D. N. Wang, W. Jin, H. L. Ho, and J. Ju, "Mode field profile and polarization dependence of long-period

fiber gratings written by CO2 laser," Opt. Commun. **281**, 2522–2525 (2008).
11. R. Slavik, "Coupling to circularly asymmetric modes via long-period gratings made in a standard straight fiber," Opt. Commun. **275**, 90–93 (2007).
12. D. D. Davis, T. K. Gaylord, E. N. Glytsis, and S. C. Mettler, "CO_2 laser-induced long-period fiber gratings: spectral characteristics, cladding modes and polarization independence," Electron. Lett. **34**, 1416–1417 (1998).
13. M. Yan, S. Y. Luo, L. Zhan, Z. M. Zhang, and Yuxing Xia, "Triple-wavelength switchable Erbium-doped fiber laser with cascaded asymmetric exposure long-period fiber gratings," Opt. Express **15**, 3685–3691 (2007).
14. B. Lee, J. Cheong, and U. Paek, "Spectral polarization-dependent loss of cascaded long-period fiber gratings," Opt. Lett. **27**, 1096–1098 (2002).
15. T.-J. Ahn, B.-H. Kim, B. H. Lee, Y. Chung, U. C. Paek, and W.-T. Han, "Torsion sensing characteristics of optical fiber with a long-period grating pair," Proc. SPIE **4579**, 154–161 (2001).
16. T. Hirose, K. Saito, S. Kojima, B. Yao, K. Ohsono, S. Sato, K. Takada, and A. J. Ikushima, "Fabrication of long-period fiber grating by CO_2 laser-annealing in fiber-drawing process," Electron. Lett. **43**, 443–445 (2007).
17. H. S. Ryu, Y. Park, S. T. Oh, Y. Chung, and D. Y. Kim, "Effect of asymmetric stress relaxation on the polarization-dependent transmission characteristics of a CO_2 laser-written long-period fiber grating," Opt. Lett. **28**, 155–157 (2003).
18. B. H. Kim, Y. Park, T.-J. Ahn, D. Y. Kim, B. H. Lee, Y. Chung, U. C. Paek, and W.-T. Han, "Residual stress relaxation in the core of optical fiber by CO_2 laser irradiation," Opt. Lett. **26**, 1657–1659 (2001).
19. B. L. Bachim and T. K. Gaylord, "Polarization-dependent loss and birefringence in long-period fiber gratings," Appl. Opt. **42**, 6818–6823 (2003).